A&A 371, 61–67 (2001)
DOI: 10.1051/0004-6361:20010308

Astronomy & Astrophysics

On the hadronic beam model of TeV γ-ray flares from blazars

D. Purmohammad[1] and J. Samimi[1,2]

[1] Department of Physics, Sharif University of Technology, PO Box 11365-9161, Tehran, Iran
e-mail: dpu@mehr.sharif.ac.ir
[2] Center for Theoretical Physics and Mathematics, PO Box 11365-8486, Tehran, Iran

Received 5 July 2000 / Accepted 5 February 2001

Abstract. We propose two models, based on the hadronic beam-cloud collision, for production of TeV γ-ray flares in blazars. In the first model, a change in bulk Lorentz factor of the jet of the Active Galactic Nucleus (AGN) produces the flare. In the second model we consider a two-stage mechanism for high-energy particle acceleration in the jet. This system produces a power law spectrum with two different power indices at low and high energies, which is more efficient than one-stage shock acceleration at high energies. Using this spectrum in a hadronic beam-cloud model for γ-ray emission of blazars, a variable TeV as well as a stable GeV γ-ray flux is predicted. The break energy in the spectrum, related to distance between the jet base and terminal shock or boundary layer thickness, is the parameter used to obtain TeV flares.

Key words. gamma rays: theory – galaxies: jets – Bl Lacertae objects: individual: Mrk 421 – acceleration of particles

1. Introduction

Blazars are a subgroup of Active Galactic Nuclei (AGN) with variable nonthermal radiation. They are believed to have a central engine, supposed to be a supermassive black hole, an accretion disk, and a relativistic jet in the axis of the disk. The jet has a bulk Lorentz factor $\geq$10 and its axis is very close to the line of sight, in many cases exhibiting superluminal motion. Although the origin of the jet is still uncertain, they are predicted to be powerful sources of cosmic ray acceleration through their terminal shocks (Rachen & Biermann 1993) or side boundaries (Ostrowski 1990) or internal oblique shocks (Lind et al. 1989). Two famous BL Lacertae, Mrk 421 and Mrk 501 are among the first blazars observed in TeV γ-ray (Punch et al. 1992; Quinn et al. 1996). The EGRET detector, operating onboard the Compton Observatory, also detected GeV γ-rays from Mrk 421 (von Montigny et al. 1995) and Mrk 501 (Kataoka et al. 1999). These two objects exhibit TeV flares (Gaidos et al. 1996; Quinn et al. 1997), but during the TeV flares, the GeV photon fluxes show minor variation. On the other hand, X-ray and TeV flares are correlated (Petry et al. 2000; Maraschi et al. 1999). This is often interpreted as a strong argument in favor of the so-called Synchrotron Self Compton (SSC) model in which ultrarelativistic electrons generate synchrotron radiation which undergo inverse compton scattering off electrons producing TeV photons (Ghisellini et al. 1985). However, this does not yet rule out the possibility of hadronic jet models in which high energy photons are produced by protons of the jet. The popular hadronic model is a Proton Initiated Cascade (PIC) mechanism proposed by Mannheim & Biermann (1992) in which protons assumed existing in the jet are accelerated to high energies and interact with the synchrotron photon field of coexisting electrons to produce mesons (mainly pions). Secondary $e^{\pm}$ pairs and photons are then generated from the decay of mesons. In this model, *pp* interactions have a negligible contribution to pion production due to low gas density in the jet. For a central black hole of mass 10^8 $M_{\odot}$ one can obtain a density less than 10^3 cm^{-3} and relative luminosity $\frac{L(pp)}{L(p\gamma)} < 10^{-5}$ at one parsec from the AGN (Mannheim 1993). Dar & Laor (1997) proposed an alternative hadronic model in which protons of the jet collide with high-density clouds ($n = 10^{10}$–10^{12} cm^{-3}) in Broad Line Regions (BLR). In the jet-cloud model, *pp* interactions can dominate photomeson cooling of the protons. The clouds pass the jet frequently so that the stationary state of γ-ray emission is a composition of a series of rapid flares. Actually, the emission from Mrk 421 sometimes goes to zero with no underlying baseline emission, which is not the case in Mrk 501 (Quinn et al. 1997). OB stars' wind is also considered as a possible target in some models (Bednarek & Protheroe 1997). In these models, it is customary to assume a power law energy spectrum for protons in the jet. The power index for this spectrum is

Send offprint requests to: J. Samimi,
e-mail: samimi@physics.sharif.ac.ir

often taken as $2 \leq \alpha \leq 3$, which comes from diffusive shock acceleration models (Drury 1983). The same power index for particles accelerated in oblique shocks is obtained, but the acceleration time scales are much smaller and hence the process is more efficient (Ostrowski 1988). Although there is at present no theory which is able to predict the spectrum of particles accelerated in a magnetic reconnection mechanism, the total effect of random reconnections may also produce a power law spectrum (Colgate 1995). In this paper we consider two models for production of TeV γ-ray flares in blazars. In the first model, a change in bulk Lorenz factor of the jet enhances the flux of TeV photons. With a suitable choice of initial and final Lorentz factors, TeV flares are obtained with insignificant variation in GeV flux. The other model involves a mechanism of particle acceleration in the jet. In this model, a two-stage acceleration system is proposed; in the first stage, particles are accelerated to form a power law spectrum with power index α_1 up to maximum energy E_2, and in the second stage they are accelerated with power index α_2. Here we specifically consider the effect of cosmic ray acceleration in the side boundary of the jet (Ostrowski 1990, 1998). It will be shown that the effect of this modification can produce both high state and low state fluxes in the TeV region, leaving GeV flux almost unchanged.

2. Hadronic jet-cloud model for TeV γ-ray emission from blazars; effect of bulk Lorentz factor variation

In this model, a collimated jet of hadronic matter emerging from a central AGN is considered. The mechanism of the jet formation is still not known with certainty, however from multiwavelength analysis of data (Petry et al. 2000; Tavecchio et al. 1998) and recent radio observations (Piner et al. 1999), its Lorentz factor is estimated to be $10 \leq \Gamma \leq 30$. Begelman et al. (1994) have obtained larger values of $\Gamma \sim 30$–100 from energy constraints of such a jet.

Due to their line-shapes, relative strengths and time-lag response to variations with time of the central continuum source, BLRs seem to consist of Broad Line Clouds of size 10^{11}–10^{14} cm and hadronic density of 10^{10}–10^{12} cm^{-3} moving with high random velocities (Peterson 1993). When these clouds pass through the beam, hadronic interaction between protons of the jet and cloud produces high energy γ-rays as well as electrons, muons and neutrinos. Looking for correlated neutrino and TeV γ-ray flux variations from these blazars has been suggested as an observational test for this model (Dar & Shaviv 1996). The electrons also can emit synchrotron radiation and cause correlated X-ray flares. For a power law spectrum for protons in the jet, according to the scaling hypothesis, the spectrum of electrons and neutrinos would be a power law, too.

The emissivity of γ-rays in the jet-cloud region is:

$$q(E_\gamma) = n_\mathrm{c} \int_{E_\mathrm{th}}^{\infty} \mathrm{d}E_\mathrm{p}\, I_\mathrm{p}(E_\mathrm{p}) \frac{\mathrm{d}\sigma}{\mathrm{d}E_\gamma}(E_\gamma, E_\mathrm{p}) \tag{1}$$

where E_p and E_γ are proton and photon energies respectively, n_c is density of the target protons in the cloud, I_p is the flux of protons in the jet, $\frac{\mathrm{d}\sigma}{\mathrm{d}E_\gamma}$ is the cross section for inclusive production of high energy photons in pp collision and E_th is threshold energy of the proton to produce a photon with E_γ. For the cross section we use (Dar & Laor 1997):

$$\frac{E_\mathrm{p}}{\sigma_\mathrm{in}} \frac{\mathrm{d}^3\sigma}{\mathrm{d}p_\mathrm{t}^2 \mathrm{d}E_\gamma} \simeq \frac{c}{E_0} \frac{\exp\left(-cp_\mathrm{t}/E_0\right)}{2\pi p_\mathrm{t}} f(x) \tag{2}$$

where p_t is transverse momentum of the photon, $E_0 \simeq 0.16\,\mathrm{GeV}$ and $\sigma_\mathrm{in} \simeq 35\,\mathrm{mb}$ and $f(x) = (1-x)^3/\sqrt{x}$ which is a function of $x(\equiv E_\gamma/E_p)$ only. Exponential dependence on p_t beams the γ-ray production into very small angles relative to the proton direction. So we approximate the emerging photon direction by the initial proton direction ($\theta_\gamma \approx \theta_p$). Integrating over transverse momentum gives $\frac{\mathrm{d}\sigma}{\mathrm{d}x} \simeq \sigma_\mathrm{in} f(x)$.

To be consistent with the diffusive acceleration model, an isotropic power law distribution for protons is assumed in the comoving frame of the jet (Ostrowski 1990), $I'_\mathrm{p} = cn'(E'_\mathrm{p}, \theta'_\mathrm{p}) = \frac{cA}{4\pi} E'^{-\alpha}_\mathrm{p}$, where n' is density of protons having energy E'_p and their direction of motion has an angle θ'_p with the jet axis in the comoving frame of the jet. Actually, some leptonic models also make this assumption (Dermer et al. 1992). Transforming to the AGN frame:

$$n(E_\mathrm{p}, \theta_\mathrm{p}) = \frac{A\Gamma^{-(\alpha-1)} \left(E_\mathrm{p} - \beta\cos\theta_\mathrm{p}\sqrt{E_\mathrm{p}^2 - m_\mathrm{p}^2c^4}\right)^{-\alpha}}{4\pi \left(\sin\theta_\mathrm{p}^2 + \Gamma^2 \left(\cos\theta_\mathrm{p} - \frac{\beta E_\mathrm{p}}{\sqrt{E_\mathrm{p}^2 - m_\mathrm{p}^2c^4}}\right)^2\right)^{1/2}} \tag{3}$$

where unprimed quantities are in the AGN frame, Γ is the bulk Lorentz factor of the jet, $\beta = v/c$ and v is its bulk velocity. We will use $c\,n(E_\mathrm{p}, \theta_\mathrm{p})$ for I_p in Eq. (1).

The results of $n(E_\mathrm{p}, \theta_\mathrm{p})$ for a few selected values of the parameters are shown in Fig. 1. For very high energies $n(E_\mathrm{p}, \theta_\mathrm{p})$ is a power law distribution, but for lower energies ($E_\mathrm{p} < \Gamma m_\mathrm{p} c^2$) it has quite a different behaviour. Therefore, numeric integration is performed to obtain emissivity.

For an observer at a distance r from the source and with the line of sight making an angle θ with the jet axis, the differential photon flux (in $\mathrm{GeV}^{-1}\mathrm{s}^{-1}\mathrm{cm}^{-2}$) is:

$$N_\gamma(E_\gamma, r, \theta) = \int_{\Omega_\mathrm{c}} \mathrm{d}\Omega_\mathrm{c} \int_0^{l_\mathrm{c}} q(E_\gamma, \theta_\gamma)\,\mathrm{d}l \tag{4}$$

where Ω_c is the solid angle in which the cloud is seen; $\Omega_\mathrm{c} = \pi R^2/r^2$ and l_c is the thickness of cloud in each solid angle bin $\mathrm{d}\Omega_\mathrm{c}$. For far enough sources, $\theta_\gamma \approx \theta$ and for a spherical cloud of radius R we obtain $N_\gamma(E_\gamma, r, \theta) \approx \frac{4}{3} R\,\Omega_\mathrm{c}\, q(E_\gamma, \theta) = \frac{4\pi R^3}{3r^2}\, q(E_\gamma, \theta)$.

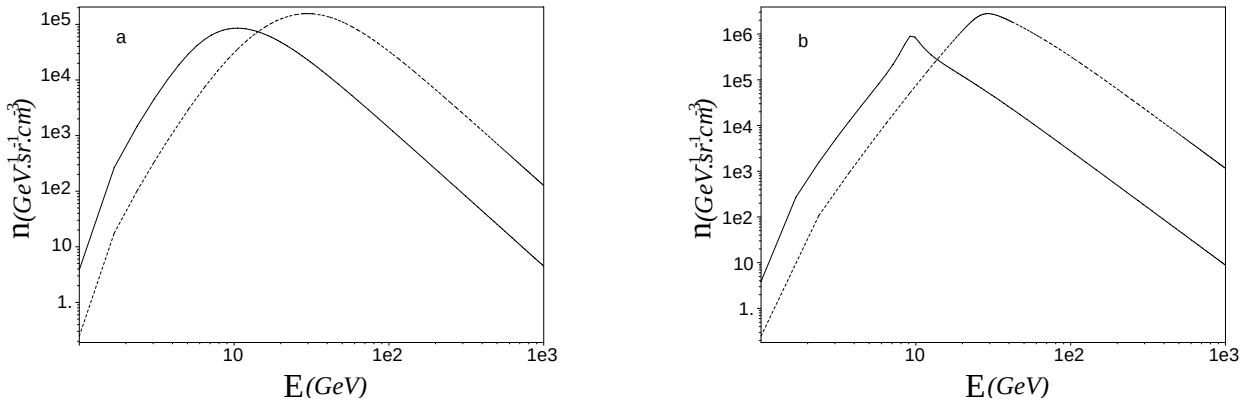

Fig. 1. Spectrum of protons in jets with $\alpha = 2.5$, $\Gamma = 10$ (solid lines) and $\Gamma = 30$ (dash lines). In **a)** $\theta = 6^\circ$ and in **b)** $\theta = 0.6^\circ$

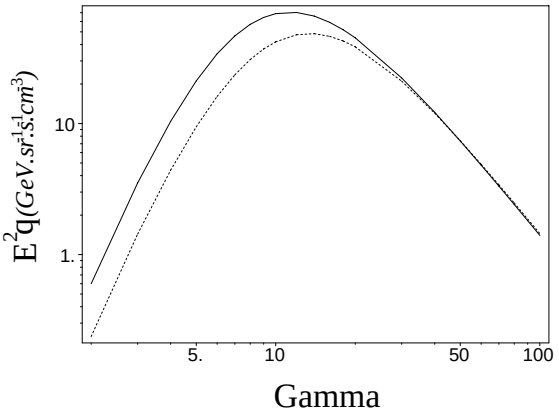

Fig. 2. Dependence of γ-ray emissivity on bulk Lorentz factor for $E_\gamma = 1$ GeV (solid line) and $E_\gamma = 1$ TeV (dashed line) and $\theta = 6^\circ$. From this plot one can find some values of Γ_1 and Γ_2 which give nearly identical emissivities at 1 GeV but different emissivities at 1 TeV

In $\log(N_\gamma)$-$\log(E_\gamma)$ plots, $\frac{4\pi}{3}R^3/r^2$ appears as an additive constant which moves the $q(E_\gamma, \theta)$ plot vertically, so for comparison of the observed spectrum of Mrk 421 with this model we just compare $q(E_\gamma, \theta)$ with data by shifting the whole data set on the vertical axis. From this shift we can choose a suitable value for R.

We will first examine the variations of the gamma ray emissivity with respect to changes in the bulk Lorentz factor of the jet. For any fixed values of E_γ and θ, the emissivity increases with Γ up to a maximum at $\Gamma_{\max}$, which depends on θ and E_γ, and decreases afterwards (Fig. 2). Because of the dependence of $\Gamma_{\max}$ on E_γ, for a fixed θ, it is possible to have two different Γ's for which a large difference occurs in $q(E_\gamma)$ at TeV energies but have an insignificant difference in the GeV range. In Fig. 3 predicted emissivities for some θ and different Γ's are presented. The data of Mrk 421 in the GeV range (Lin et al. 1994) and TeV low state (Mohanty et al. 1993; Piron 2000) and high state (McEnery et al. 1997), divided by $\frac{4\pi}{3}R^3/r^2$ are also presented as error boxes for comparison. For these calculations we used $n_c = 10^{11}$ cm^{-3}, $\alpha = 2.5$ and $A = 10^5$. The value for A is obtained by assuming a dynamo model for the jet production (Lovelace 1976), which gives the output power of the jet as a function of magnetic field in the accretion disk and mass of the black hole. Applying the Shakura & Sunyaev model (1973) to the accretion disk of a supermassive black hole one can obtain $B \leq 10^4$ Gauss for the magnetic field in the inner part of the disk. Using this value in the Lovelace dynamo model yields $L_j \leq 10^{46}$ erg s^{-1} for the output power of the jet, which is in agreement with the Begelman et al. (1994) estimation for the power of a highly collimated AGN jet. Integrating over the energy with the proton spectrum given above and equating the result to power of the jet gives $A = 10^5$. For Mrk 421 the redshift is $z = 0.03$ and with $H_0 = 65$ km s^{-1} Mpc^{-1} we have $r = 4.3\ 10^{26}$ cm. For each spectrum, the cloud radius R is calculated and given in the caption of the figure. With the selected Γ's the spectra can produce low and high states in TeV energies with a small variation in GeV energies. In Figs. 3a and 3b, although the predicted spectra are comparable with EGRET data in sub-GeV energies, in GeV energies the calculated emissivities are an order of magnitude higher than the EGRET data. The situation is reversed in Figs. 3c and 3d, where the predicted spectra are comparable to the GeV observational data, but negligible in the sub-GeV range. However, the spectra in the low energy part is harder than the EGRET data. It seems that this model, though successful in accounting for TeV flares, is not sufficient to account for production of the observed sub-GeV flux. This is also the case for our second model (see Sect. 3) as well as the Beall & Bednarek (1999) model. For low energy γ-rays, other sources have been proposed (Bednarek 1998).

3. Two-stage acceleration system for high energy protons

If a mechanism of particle acceleration in the jet produces a power law spectrum $\propto E^{-\alpha'}$ for particles in the energy range $E_1 < E < E_2$ and then these particles enter a second acceleration mechanism which can produce a power law spectrum with power index α, with $\alpha > \alpha'$, one can

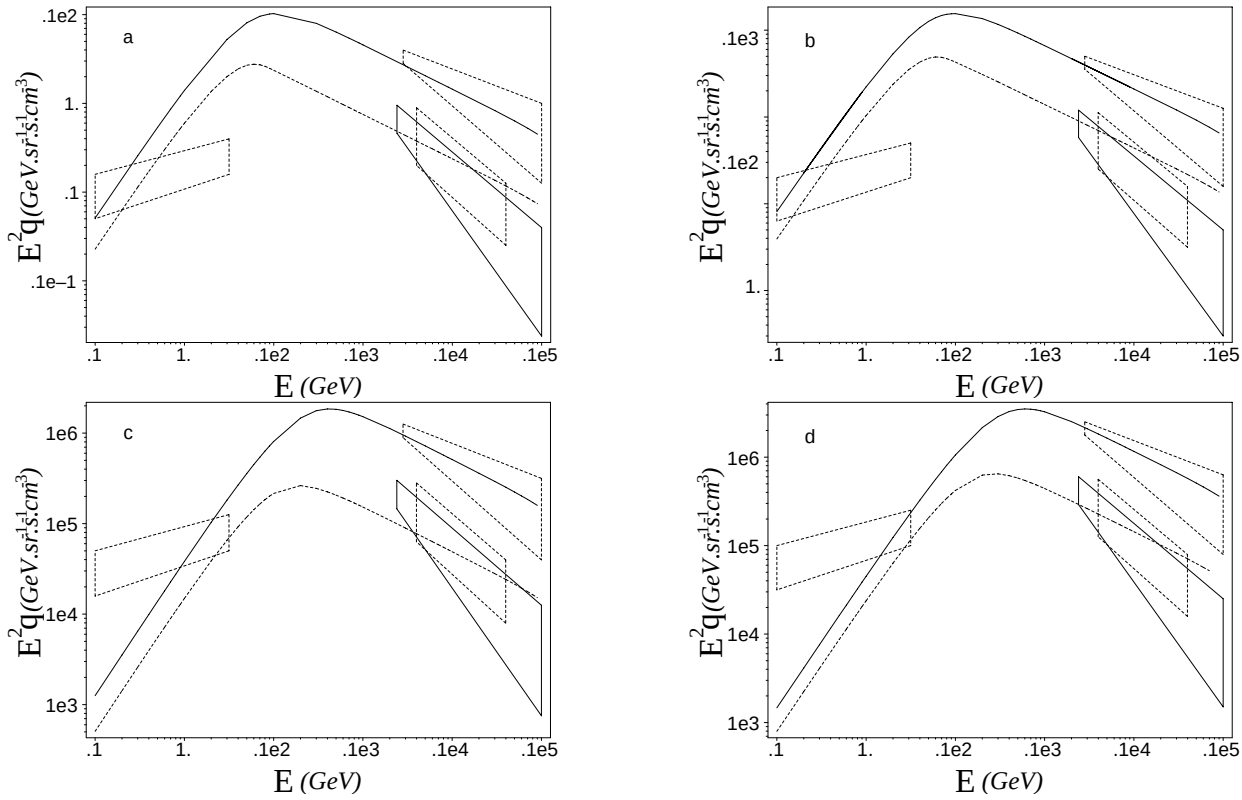

Fig. 3. The first model results: The spectra for $\theta = 6^\circ$ and different Γ's are compared to data of Mrk 421 in GeV range (Lin et al. 1994) and TeV low state (Mohanty et al. 1993; dashed box and Piron 2000; solid box) and high state (McEnery et al. 1997), as error boxes. $\Gamma_1 = 2$ (dashed line), $\Gamma_2 = 100$ (solid line) and $R = 1.7\ 10^{15}$ cm in **a)**, $\Gamma_1 = 4$ (dashed line), $\Gamma_2 = 30$ (solid line) and $R = 6.7\ 10^{14}$ cm in **b)**, $\theta = 0.6^\circ$, $\Gamma_1 = 30$ (dashed line), $\Gamma_2 = 60$ (solid line) and $R = 2.5\ 10^{13}$ cm in **c)**, $\Gamma_1 = 40$ (dashed line), $\Gamma_2 = 90$ (solid line) and $R = 2\ 10^{13}$ cm in **d)**. See Sect. 2 for details

easily show that the output of the second stage will be approximately a broken power law spectrum:

$$\frac{\mathrm{d}N}{\mathrm{d}E} \propto \begin{cases} E^{-\alpha'} & E_1 < E < E_2 \\ E^{-\alpha} & E > E_2 \end{cases} \tag{5}$$

where E_1 and E_2 are the minimum and the maximum energy available in the first stage.

A two-stage system of particle acceleration in relativistic jets in AGNs is obtained when diffusive acceleration in tangential discontinuity at the side boundaries of the jet (Ostrowski 1990) is followed by diffusive acceleration in the strong terminal shock. Semi-analytic calculations (Biermann 1993; Biermann & Strom 1993) as well as Monte Carlo simulations (Gieseler 1999) of diffusive acceleration in strong terminal shock in such a jet give $2 \leq \alpha \leq 3$. Simulations for diffusive acceleration in tangential discontinuity of the velocity field at the side boundaries of the jets give $1.5 \leq \alpha' \leq 2$ (Ostrowski 1990).

In the model considered here, the first stage of acceleration can occur in the tangential shear layer of a jet, and produce a spatially isotropic power law energy distribution in the comoving frame of the jet. After entering the terminal shock of the jet in the second stage of acceleration, the spectrum steepens as given in Eq. (5). This system will produce high energy particles more efficiently compared to a one-stage system, e.g. diffusive acceleration in the terminal shock of the jet. The maximum energy of the second stage is limited by the balance between energy gain and loss rates. For protons, loss mechanisms are mainly photomeson interactions. Actually, the maximum energy of the second stage is much higher than E_2, and for a power law spectrum, results of our calculations are not sensitive to $E_{\max}$ for $E_{\max} \gg 1$ TeV. In the first stage, E_2 depends on the size of the acceleration region, e.g. length of the jet from base to terminal shock and thickness of the side boundary layer (Ostrowski 1990, 1998). These quantities can vary when clouds pass through the jet at different distances or when the thickness of the boundary layer changes in response to variations in density of the environment around the jet. We have used E_2 as a parameter to fit our model to the data. We also chose $\alpha' = 1.5$ and $\alpha = 2.5$. The former is taken from simulation results for ultrarelativistic jets (Ostrowski 1990), and the latter comes from TeV γ-ray data of Mrk 421 (Zweerink et al. 1997; Djannati-Atai et al. 1999) as well as diffusive shock acceleration theory.

Figure 4 shows results of our second model for some selected values of Γ, E_2 and θ. In all of the computations for this model, we have used $n_{\mathrm{c}} = 10^{11}$ cm^{-3}, $\alpha' = 1.5$, $\alpha = 2.5$, $A = 10^5$. Data boxes are also presented as in previous plots. Values of R are calculated and given in the caption of the figure. With changing E_2 from 100 GeV to

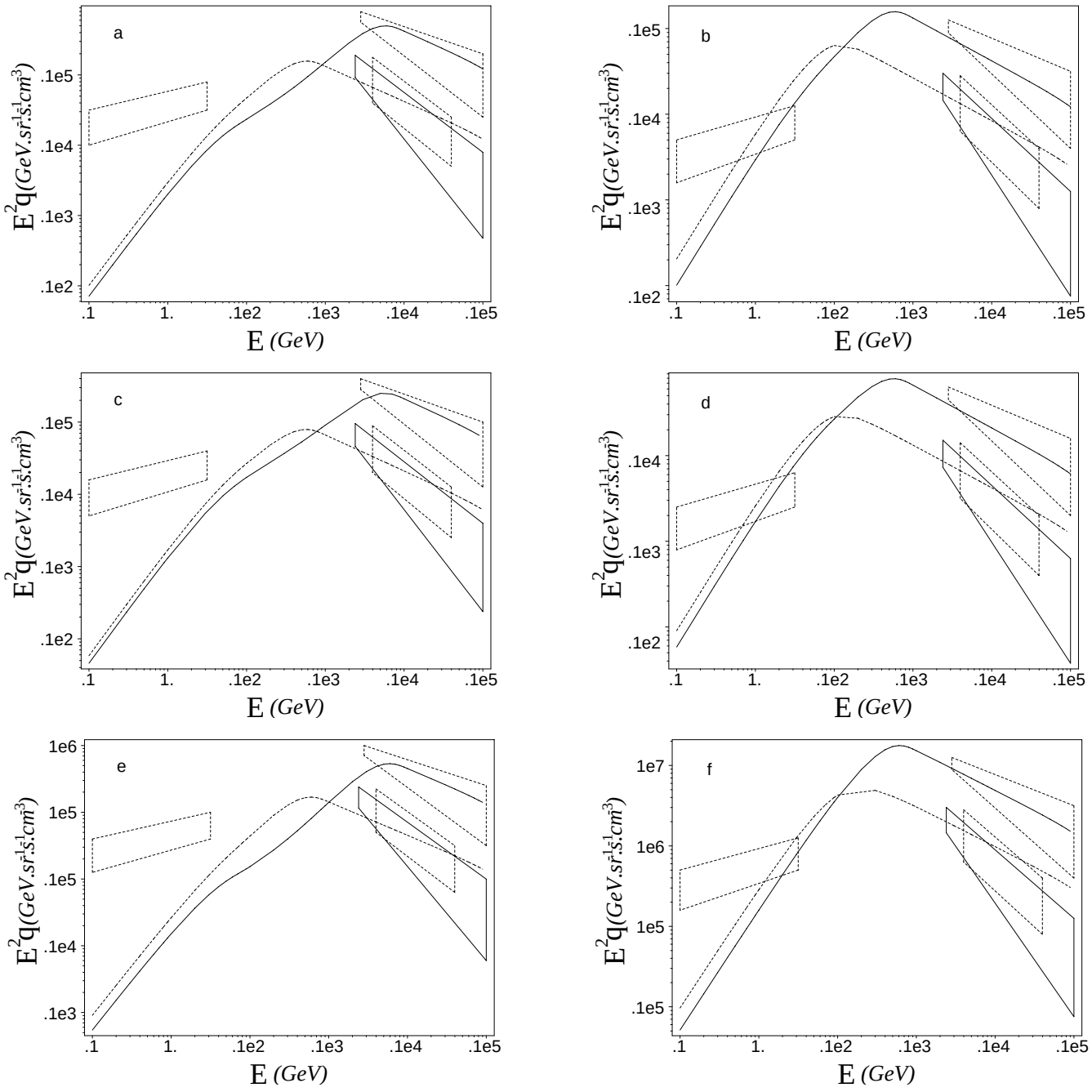

Fig. 4. The second model results: Predicted spectra for $\theta = 6°$, $\Gamma = 10$, $E_2 = 100$ GeV (dashed line), $E_2 = 1000$ GeV (solid line) and $R = 6.5\ 10^{13}$ cm in **a)**, $E_2 = 100$ GeV (solid line), $E_2 = 20$ GeV (dashed line) and $R = 1.2\ 10^{14}$ cm in **b)**, $\Gamma = 30$, $E_2 = 100$ GeV (dashed line), $E_2 = 1000$ GeV (solid line) and $R = 7.5\ 10^{13}$ cm in **c)**, $E_2 = 100$ GeV (solid line), $E_2 = 20$ GeV (dashed line) and $R = 1.5\ 10^{14}$ cm in **d)**, $\Gamma = 10$, $\theta = 0.6°$, $E_2 = 100$ GeV (dashed line), $E_2 = 1000$ GeV (solid line) and $R = 2.7\ 10^{13}$ cm in **e)**, $\Gamma = 30$, $\theta = 0.6°$, $E_2 = 100$ GeV (solid line), $E_2 = 20$ GeV (dashed line) and $R = 1.2\ 10^{13}$ cm in **f)** are compared to data of Mrk 421 as in Fig. 3. See Sect. 3 for details

1000 GeV, in each case, the model produces two spectra with good agreement to TeV low and high states, respectively, but it yields negligible flux at GeV and sub-GeV range compared to EGRET data. By changing E_2 from 20 GeV to 100 GeV, the spectra have low and high states at TeV as before and become comparable to EGRET data at GeV energies, although not the case in sub-GeV range. The spectra in low energy part is harder than the EGRET data. This discrepancy was also encountered in our first model (Sect. 2), as well as in the "collisionless loss model" of Beall & Bednarek (1999). Their conclusion that other sources for GeV γ-ray production (e.g. leptonic) are needed is confirmed by our calculations. Because of high variability in secondary $e^{\pm}$ pair flux above 10 GeV, these pairs are not the source. Scattering of nonvariable, soft X-ray photons by secondary pairs below 10 GeV could

explain the data in the GeV range. A possible source of the photons is the inner part of the accretion disk (Bednarek 1998).

4. Discussion and concluding remarks

To produce TeV γ-ray flares from blazars, two models based on hadronic beam-cloud collisions are proposed. In the first model an abrupt increase in the bulk Lorentz factor of the jet can generate a flare for $E_\gamma \geq 1\,\mathrm{TeV}$. Although the predicted spectra have less variation in low energy compared to TeV flares, they are harder than the EGRET data. In the second model, acceleration in the jet produces a broken power law spectrum for protons. The break energy, E_2, depends on the maximum energy available for a particle in diffusive acceleration in the side boundary layer of the jet, which is related to the distance of the jet base to the terminal shock or the thickness of the boundary layer (Ostrowski 1990, 1998). A sudden increase in E_2 can also generate a TeV γ-ray flare.

In both models, the flux of GeV photons undergoes little variation compared to TeV flux, but the predicted spectrum is harder than that observed. Another stable GeV source which can compensate for this deficiency is the inverse Compton scattering of soft X-ray photons coming from the inner part of the accretion disk by secondary $e^{\pm}$ pairs below 10 GeV produced in the jet-cloud region.

Both models produce a break in the gamma-ray energy spectrum in the 10–100 GeV range, which is in agreement with Beall & Bednarek's results (1999). It should be mentioned that the physical basis of our first model differs from the one given by Beall and Bednarek. They considered generation of plasma instabilities in the collision of jet and cloud as a loss mechanism for high energy particles. They assumed that the jet consists of a beam of protons with a power law energy distribution, and its Lorentz factor is attenuated when it passes through the cloud as a result of collisionless loss mechanism. The attenuation length depends on the initial Lorenz factor, density of particles in the cloud and the jet and the temperature of cloud. They produced low and high states in TeV γ-ray emission by considering the different lengths as the beam passes through the cloud. In particular, they could explain the TeV flares by a sudden change of the cloud length. In our model, such a loss mechanism is not considered; instead the change in bulk Lorenz factor of the jet is assumed to happen in the entire collision region and to be caused by the central engine.

It is worth remarking that for diffusive acceleration mechanisms mentioned in this paper, particle acceleration time scales are of the order of several gyroperiod (Hillas 1984). The acceleration time scale $t_{\mathrm{acc}} \sim T_{\mathrm{gyro}} = 10^4\ E\,(\mathrm{GeV})\ B^{-1}\ (\mathrm{Gauss})$ for a particle with energy E in a magnetic field B is much shorter than flaring time scales, as will be clear from the following argument. Correlated X-ray and γ-ray flares allow us to assume that they are generated in the same region in the jet. Secondary pairs are responsible for synchrotron emission in X-ray during flares, and they have a spectrum similar to the γ-ray spectrum due to scaling hypothesis (Dar & Shaviv 1996). So the spectrum of the secondary $e^{\pm}$ would have a break E_{b} in the 10–100 GeV region. This should result in a break ϵ_b in the synchrotron spectrum which allows us to estimate the magnetic field strength in the emission region; $B(\mathrm{Gauss}) = 1.4\ 10^4\,\epsilon_{\mathrm{b}}(\mathrm{KeV}) E_{\mathrm{b}}^{-2}(\mathrm{GeV})$. A break in synchrotron emission from Mrk 421 has been observed at 1.65 KeV (Takahashi et al. 1996) which yields $B \approx 2$ Gauss. Tavecchio et al. (1998) obtained a value for B an order of magnitude smaller in the emission region of Mrk 421, assuming a SSC model. With a PIC model, Mannheim (1993) gives a 90 Gauss magnetic field for the region. With a magnetic field of the order of one Gauss, acceleration time scales less than 10 sec are obtained for the most energetic particles considered in this work. Actually, the time scales are much smaller because the acceleration takes place in regions closer to the AGN before particles enter into the emission region, and the magnetic fields in the jet vary as $B_{\parallel} \propto r^{-2}$ and $B_{\perp} \propto r^{-1}$ for components parallel and transverse to the jet, respectively (Blandford & Königl 1979). So, the field strength is higher in the acceleration regions, resulting in very short acceleration time scales. On the other hand, the minimum duration reported for TeV flares is about 15 min. (There is also evidence for x-ray flares of about 200 s from Mrk 501, Catanese & Sambruna 2000, however at the time of occurance of this flare there were no overlapping TeV observations.) The observed flare time implies that whatever change in the source which caused the flare (a change in the length of the cloud in Beall and Bednarek's model, a change in bulk Lorentz factor in our first model, or a change in the distance of the terminal shock from the base of the jet in our second model) occurs on a time scale of $2\Gamma_{\mathrm{jet}}^2 \Delta t_{\mathrm{obs}}$, which is of the order of several days. Thus the acceleration time scales are much shorter than flare time scales and this justifies our time-independent approach for the calculation of the spectra. Furthermore, a time scale of a few days for a change in the source is not extraordinary. For comparison, we note that the bulk velocity of corona mass ejections in the sun are observed to change by more than a factor of two in several days (von Rosenvinge et al. 1999). The change in the bulk Lorentz factor of the jet considered in our first model could be viewed as an ultra-relativistic analog of the velocity change in corona mass ejections.

Following the arguments of Kerrick et al. (1995), we note that the extreme upper limit for the size of the emission region of a relativistic jet moving toward the observer is $2c\Gamma_{\mathrm{jet}}^2 \Delta t_{\mathrm{obs}}$. For the jets considered here, assuming $\Delta t_{\mathrm{obs}} \sim 15$ min, this is 10^{15-16} cm, which is consistent with the upper limit for our cloud sizes which are in the range of 10^{13-15} cm. It is also important to note that 15 min is a limit of photon statistics and the actual TeV flare time could be much shorter. However, even for a flare of one or two orders of magnitude shorter, some of our results for cloud sizes are still acceptable.

The hadronic jet-cloud models discussed here have two simply-inferred predictions which can be tested in the future observations of TeV flares from Mrk 421 and Mrk 501: (a) The TeV light curves of the flares, unlike the corresponding x-ray flares, should be almost symmetric (i.e. equal rise time and fall time), independent of geometry of the clouds. Obviously, the total flare time could be more than twice the rise time. (b) Since the rise time of a flare is an indicator of the cloud size, and for spherical clouds smaller than the jet diameter, TeV peak luminosity is proportional to the cloud volume, and our models predict $L_{\rm TeVflare} \propto t^3_{\rm rise}$. If the target matter has a spherical shell configuration around the AGN, the luminosity will be proportional to the thickness of the part of shell which intercepts the jet and hence $L_{\rm TeVflare} \propto t_{\rm rise}$.

Acknowledgements. Authors would like to express their thanks to D. Bhattacharya and F. Sheikhmomeni for their useful discussions. We also acknowledge anonymous referees for their numerous constructive comments. This research has been partly supported by Grant No. NRCI 1853 of National Research Council of Islamic Republic of Iran.

References

Beall, J. H., & Bednarek, W. 1999, ApJ, 510, 188
Bednarek, W. 1998, MNRAS, 294, 439
Bednarek, W., & Protheroe, R. J. 1997, MNRAS, 287, L9
Begelman, M. C., et al. 1994, ApJ, L57
Biermann, P. L. 1993, A&A, 271, 649
Biermann, P. L., & Strom, R. G. 1993, A&A, 275, 659
Blandford, R. D., & Königl, A. 1979, ApJ, 232, 34
Colgate, S. A. 1995, in Proc. 24th ICRC (Rome), 3, 341
Catanese, M., & Sambruna, R. M. 2000, ApJ, 534, L39
Dar, A., & Laor, A. 1997, ApJ, 478, L5
Dar, A., & Shaviv, N. J. 1996, Astropart. Phys., 4, 343
Dermer, C. D., et al. 1992, A&A, 256, L27
Djannati-Atai, A., et al. 1999, A&A, 350, 17
Drury, L. O'C. 1983, Rep. Prog. Phys., 46, 973
Gaidos, J. A., et al. 1996, Nature, 383, 319
Ghisellini, G., et al. 1985, A&A, 146, 204
Gieseler, U. D. J., et al. 1999, A&A, 345, 298
Hillas, A. M. 1984, ARA&A, 22, 425
Kataoka, J., et al. 1999, ApJ, 514, 138
Kerrick, A. D., et al. 1995, ApJ, 438, L59
Lin, Y. C., et al. 1994, Proc. of the 2nd Compton Symp., ed. C. E. Fichtel, N. Gehrel, & J. P. Norris (AIP, New York), No. 304, 582
Lind, K. R., et al. 1989, ApJ, 344,89
Lovelace, R. V. E. 1976, Nature, 262, 649
Mannheim, K. 1993, A&A, 269, 67
Mannheim, K., & Biermann, P. L. 1992, A&A, 253, L21
Maraschi, L., et al. 1999, Astropart. Phys., 11, 189
McEnery, J. E., et al. 1997, Proc. 25th ICRC (Durban), OG 4.3.4,
Mohanty, G., et al. 1993, in Proc. 23th ICRC (Calgary), V. 1, p. 440
Ostrowski, M. 1988, MNRAS, 233,257
Ostrowski, M. 1990, A&A, 238, 435
Ostrowski, M. 1998, A&A, 335, 134
Peterson, B. M. 1993, PASP, 105, 247
Petry, D., et al. 2000, ApJ, 536, 742
Piner, B. J., et al. 1999, ApJ, 525,176
Piron, F. 2000, for the CAT collaboration, ed. B. L. Dingus, M. H. Salamon, & D. B. Kieda, AIP Conf. Proc., 515, 113
Punch, M., et al. 1992, Nature, 106, 477
Quinn, J., et al. 1996, ApJ, 456,L83
Quinn, J., et al. 1997, in Proc. 25th ICRC (Durban), OG 4.3.3,
Rachen, J. P., & Biermann P. L. 1993, A&A, 272, 161
Shakura, N. I., & Sunyaev, R. A. 1973, A&A, 24, 335
Takahashi, T., et al. 1996, ApJ, 470, L89
Tavecchio, F., et al. 1998, ApJ, 509, 608
von Montigny, C., et al. 1995, ApJ, 440, 525
von Rosenvinge, T. T., et al. 1999, Proc. of 26th ICRC (Salt Lake City), 6, 131
Zweerink, J. A., et al. 1997, ApJ, 490, L141